UC Berkeley
UC Berkeley Previously Published Works

Title
Cost and carbon implications of flexible biomanufacturing to produce bio-based gasoline, jet fuel, and platform chemicals

Permalink
https://escholarship.org/uc/item/22x8r1q9

Journal
Chemical Engineering Journal, 543

ISSN
1385-8947

Authors
Baral, Nawa Raj
Eng, Thomas
Banerjee, Deepanwita
et al.

Publication Date
2026-09-01

DOI
10.1016/j.cej.2026.177641

Copyright Information
This work is made available under the terms of a Creative Commons Attribution License, available at https://creativecommons.org/licenses/by/4.0/

Peer reviewed

eScholarship.org Powered by the California Digital Library
University of California

Chemical Engineering Journal 543 (2026) 177641

Contents lists available at ScienceDirect

Chemical Engineering Journal

journal homepage: www.elsevier.com/locate/cej

Cost and carbon implications of flexible biomanufacturing to produce bio-based gasoline, jet fuel, and platform chemicals

Nawa Raj Baral [a,b,*], Thomas Eng [a,b], Deepanwita Banerjee [a,b], Blake A. Simmons [a,b], Aindrila Mukhopadhyay [a,b,c], Corinne D. Scown [a,b,d]

[a] Joint BioEnergy Institute, Lawrence Berkeley National Laboratory, Berkeley, California, 94720, United States
[b] Biological Systems and Engineering Division, Lawrence Berkeley National Laboratory, Berkeley, California, 94720, United States
[c] Environmental Genomics and Systems Biology, Lawrence Berkeley National Laboratory, Berkeley, California, 94720, United States
[d] Energy Analysis Division, Lawrence Berkeley National Laboratory, Berkeley, California, 94720, United States.

ARTICLE INFO

Keywords:
Ensiled biomass
Carboxylic acids
Ionic liquids
Biomass deconstruction
Isoprenol
Indigoidine
Synthetic fuels

ABSTRACT

Most biorefineries rely on fermentation to produce a single molecule, such as ethanol. This exposes facilities to price volatility and limits their flexibility to respond to market shifts and critical domestic supply chain needs. Reorienting biomanufacturing toward greater flexibility necessitates the development of versatile production platforms and chemicals with multiple upgrading options to broaden the suite of products. This study presents a design that leverages biomass ensiling, ionic liquid pretreatment, industrial microbial hosts, and catalytic upgrading. The result is a platform to convert sorghum to organic acids, indigoidine (an example of a polymer precursor and alternative to a textile dye), and varying ratios of gasoline and jet fuel blendstocks. The facility can reach net average profits above $111 per bone-dry metric ton of biomass, but only if industrial-grade organic acids are recovered and indigoidine can be used as a one-to-one replacement for synthetic indigo dye at current market prices. Results further demonstrate that economic performance is strongly governed by product allocation decisions, particularly the balance between fuels and higher-value chemical products. Rather than relying on single-product optimization, this work highlights a portfolio-based production strategy that enables dynamic adjustment of product outputs in response to market conditions. Overall, the integrated use of flexible feedstock processing, multiproduct upgrading, and selective valorization pathways provides a framework for improving the economic resilience and adaptability of future lignocellulosic biorefineries.

1. Introduction

A key value proposition for expansion of biorefineries and biomanufacturing is their ability to satisfy a variety of fuel and chemical production needs, relying primarily on domestic resources such as lignocellulosic biomass, starches, and sugars [1–3]. However, with its focus squarely on maximizing profits in the highly competitive and low-profit-margin fuel and commodities markets, most fermentation facilities have prioritized the production of single molecules, such as ethanol [4] and lactic acid [5]. This raises the question of whether a biomanufacturing platform built for greater flexibility can compete and what strategies might enable it to be both responsive and efficient.

Most prior technoeconomic analysis (TEA) and life-cycle assessment (LCA) studies have focused on either maximizing conversion of carbon in polysaccharides in biomass to salable products [4] or maximizing conversion of carbon in both polysaccharides and lignin [2,3,6,7]. More recent studies have expanded toward integrated biorefineries producing fuels and chemicals [8–10]; however, these systems are still typically evaluated under single-product or limited-co-product optimization frameworks, with relatively little exploration of dynamic product allocation or portfolio-based design strategies. At the same time, recent advances in catalytic and reaction-environment engineering demonstrate that biomass- and CO_2-derived intermediates can be selectively converted into diverse value-added products with high efficiency, highlighting the technical feasibility of flexible, multiproduct conversion platforms [11–13]. In contrast to these prior approaches, this work explicitly evaluates a multiproduct optimization framework that enables simultaneous production of fuels, platform chemicals, and specialty products under varying allocation ratios, thereby extending beyond conventional single-objective TEA/LCA studies.

* Corresponding author at: Joint BioEnergy Institute, Lawrence Berkeley National Laboratory, Berkeley, California, 94720, United States.
E-mail address: nrbaral@lbl.gov (N.R. Baral).

https://doi.org/10.1016/j.cej.2026.177641
Received 6 February 2026; Received in revised form 5 May 2026; Accepted 22 May 2026
Available online 23 May 2026
1385-8947/© 2026 The Authors. Published by Elsevier B.V. This is an open access article under the CC BY license (http://creativecommons.org/licenses/by/4.0/).

This focus on efficient conversion does not account for the value of flexibility, which is difficult to quantify. There may be strategically-valuable molecules with unique or emerging applications, like indigoidine [6], that may need to be scaled up on short notice. However, continuous large-scale production of such specialty chemicals could quickly flood the global market if treated as a primary output, and is therefore more appropriately considered within a flexible product portfolio rather than a standalone production target. In this study, indigoidine is therefore used as a representative example of a high-value, emerging product class rather than a target for full displacement of existing dye markets. This study seeks to design and analyze lignocellulosic biorefinery configurations that balance efficient conversion with the need to offer more flexible biomanufacturing for future domestic supply chains. Accordingly, the focus is on evaluating product portfolio flexibility and dynamic allocation among fuels, platform chemicals, and specialty products, rather than optimizing around any single surrogate molecule.

Along the entire biomanufacturing supply chain, there are various opportunities to extract value. The key is in identifying which opportunities yield benefits that outweigh their costs. Some biomass may either naturally contain sufficient levels of compounds that can be extracted and sold, or may be modified to accumulate them [14,15]. The biomass storage process itself can yield potential products, as biomass ensiling is a common storage method [16] and the ensiling process naturally generates carboxylic acids, including acetic, lactic, and butyric acids, which can aid in biomass pretreatment processes and can themselves be recovered as products [17,18]. Once biomass is delivered to the biomanufacturing facility, it is possible to deconstruct and convert it to targets that are valuable targets and also function as platform chemicals that can be upgraded to other products.

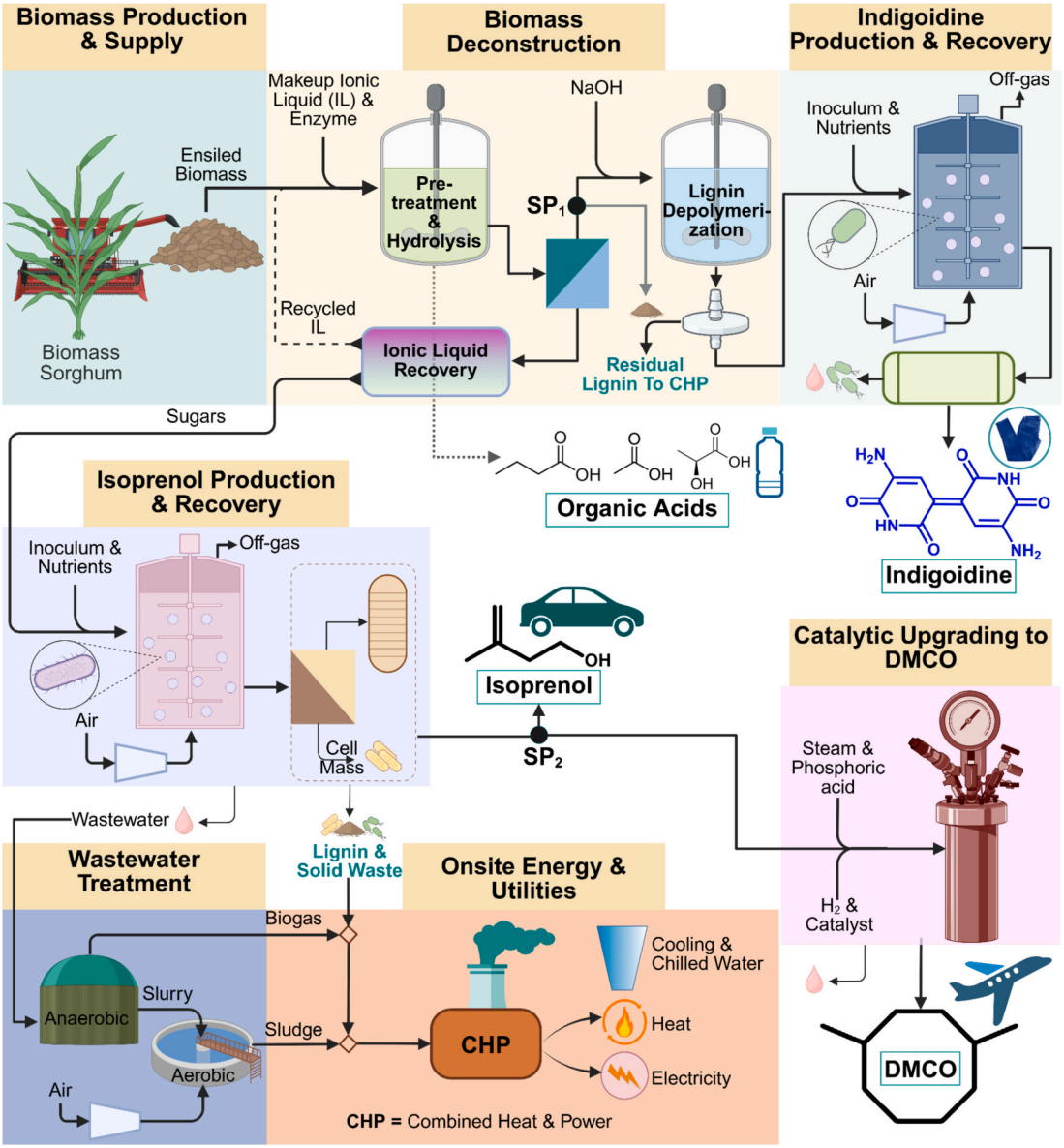


Fig. 1. An overview of the multiproduct biorefinery considered in this study. This model biorefinery integrates biomass sorghum production, supply, and conversion into isoprenol, 1,4-dimethylcyclooctane (DMCO), indigoidine, and organic acids, primarily acetic and lactic acids, as the main products. This modeled biorefinery allows for product adjustments. Specifically, isoprenol can be used as a gasoline blendstock or upgraded into DMCO. Similarly, lignin can be diverted to indigoidine production or sent to onsite heat and power generation. **SP_1** represents separation point 1, where part of the solid fraction is sent to the lignin depolymerization unit and the remainder is used for onsite heat and power generation. **SP_2** represents separation point 2, where part isoprenol is stored onsite for direct use and the remainder catalytically upgraded to DMCO. The detailed modeling data, including the process flow sheet, material inputs, equipment sizing, and cost estimates, are available in the Project PISCES database [28].

To probe the hypothesis that a multiproduct biorefinery can compete with single-product facilities and identify optimal product ratios, we designed and simulated a biorefinery capable of taking ensiled sorghum biomass and producing varying ratios of gasoline blendstock, jet fuel blendstock, and high-value specialty chemicals in different ratios (Fig. 1). Specifically, the envisioned facility produces isoprenol, 1,4-dimethylcyclooctane (DMCO), indigoidine, and three organic acids. Isoprenol is biologically produced from biomass-derived sugars [19–21] and serves as a gasoline blendstock or can be upgraded into isoprene, a precursor to synthetic rubber used in tires. Isoprenol can also be upgraded to high energy-density jet fuel blendstock, DMCO (9.2% higher energy density than Jet-A), using a low-cost iron-based catalyst [22]. A portion of the lignin stream is depolymerized and diverted for biological production of indigoidine [6,23] while the remaining fraction is used onsite for heat and power generation. Indigoidine has applications in textile dyeing, food coloring, and manufacturing bio-transistors [24–27]. Acetic, lactic, and butyric acids are all naturally produced as part of the biomass ensiling process [17], which can be recovered after biomass pretreatment.

This study addresses open questions regarding the conditions under which biorefineries can achieve price and lifecycle CO_2 emissions parity with petroleum-based processes, at the currently demonstrated product yields. In doing so, it provides a systematic comparison of multiproduct allocation strategies within a unified TEA and LCA framework, complementing prior studies that have primarily focused on single-product optimization or fixed coproduct configurations. We evaluate the implications of maintaining demonstrated yields at commercial scale, achieving high recovery of organic acids, and the strategic allocation of lignin toward co-product generation. The analysis considers trade-offs in product diversification and the potential for an adaptive biomanufacturing framework in which versatile platform chemicals and high-value co-products are produced from a single biomass feedstock to enhance economic viability.

2. Methods

2.1. Process model development

We designed and modeled both single-product and multiproduct biorefineries using the SuperPro Designer software [29]. The detailed modeling data, including the process flow sheet, material inputs, equipment sizing, and cost estimates, are documented in our publicly accessible data-sharing platform (Project PISCES) [28]. The modeled biorefinery processes 2000 bone-dry metric tons (bdt) of biomass sorghum per day (Fig. 1). The moisture content of delivered ensiled biomass sorghum is assumed to be 60% [16]. We considered a typical biomass harvesting and supply system as documented in a prior study [16]. In this system, biomass sorghum is harvested using a forage harvester, directly loaded into a box truck, transported to the biorefinery, and ensiled adjacent to the biorefinery prior to use [16]. The biomass trucking distance is calculated assuming that 5% of the land around the biorefinery is sorghum fields [16], with a biomass sorghum yield of 22.4 metric tons per hectare (10 tons per acre) [30].

The biomass ensiling process not only prevents aerobic degradation of biomass sorghum due to its high moisture content but also generates carboxylic acids—such as acetic acid, lactic acid, and butyric acid—in concentrations ranging from 8% to 11% [17]. In addition, the selection of ensiled biomass is supported by prior studies [17,18] showing that ensiling alters biomass physicochemical properties in a way that improves downstream deconstruction efficiency, including reduced pretreatment severity (lower ionic liquid and enzyme requirements) and enhanced sugar and product yields compared to dry sorghum. These advantages arise from partial structural disruption during the ensiling process and the presence of fermentation-derived organic acids, which collectively improve biomass accessibility and conversion performance.

The organic acid-rich ensiled biomass feedstock is conveyed from storage piles to the biomass deconstruction unit, where it undergoes pretreatment with cholinium lysinate ([Ch][Lys]), an ionic liquid (IL) [17]. Compared to conventional pretreatment methods such as dilute acid, hydrothermal, and alkaline processes, cholinium lysinate ([Ch][Lys]) offers milder operating conditions, improved selectivity, and more effective disruption of lignocellulosic biomass [31,32]. It has demonstrated strong delignification performance and high glucose yields after enzymatic saccharification of pretreated substrates [31,33]. In addition, [Ch][Lys] is recyclable and chemically tunable, supporting process integration and sustainability [34]. It is not toxic to enzymes and microbes at a low concentration (below 10 wt%), enabling potential one-pot processing without extensive washing prior to hydrolysis [31,33]. These properties make it well suited for multiproduct biorefinery configurations requiring efficient valorization of both carbohydrate- and lignin-derived streams. Ensiled biomass is pretreated at 140 °C for 3 h with 5 wt% IL loading [17]. Following pretreatment, organic acids are recovered. We consider a conventional chemical separation approach [35,36], including flash and thin film evaporation followed by fractional distillation. However, recent developments in membrane-based water removal, followed by distillation and crystallization, could improve purity [36,37]. We assume a baseline organic acid recovery rate of 95% and also conduct a scenario analysis with a pessimistic recovery rate of 60%.

The pretreated slurry after organic acid recovery is sent to the enzymatic hydrolysis reactor. The pores formed during pretreatment enhance enzyme accessibility, resulting in glucose yield of 91.5% at a low enzyme loading rate of 10 mg-protein/g-glucan [17]. After hydrolysis, the solid and liquid fractions are separated. The liquid fraction (sugar solution) after recovery of IL is directed to the isoprenol bioconversion unit, while the solid fraction—primarily composed of insoluble lignin and unutilized cellulose and hemicellulose—is sent to the lignin depolymerization unit (Fig. 1). The IL is recovered using a pervaporation system, as demonstrated in a prior study [38].

The liquid fraction, after the recovery of the IL, primarily contains simple sugars, including glucose and xylose, which are catabolized by the bacterial production host *Escherichia coli,* to produce isoprenol [19]. Following bioconversion, isoprenol is recovered using a distillation and decantation system consistent with prior study [39], while the remaining byproducts are sent to the wastewater treatment unit.

As a baseline assumption, half of the recovered isoprenol is stored onsite for direct use as a gasoline blendstock, while the remaining portion is sent to the catalytic conversion unit for upgrading into DMCO. However, we analyzed the detailed cost and lifecycle CO_2 emissions impacts by varying the direct use of isoprenol from 1% to 99%. The isoprenol upgrading process involves the dehydration of isoprenol to produce isoprene, the dimerization of isoprene in the presence of an iron-based catalyst to form 1,6-dimethyl-1,5-cyclooctadiene (DMCOD), and the hydrogenation of DMCOD to yield DMCO [22,40]. The final DMCO product is recovered via distillation and stored onsite.

In addition to isoprenol and DMCO, indigoidine is another major product of the modeled biorefinery. It is biologically produced from lignin-derived bio-intermediates [23,41]. The process begins with the depolymerization of lignin or the solid obtained after enzymatic hydrolysis. This study considered base-catalyzed lignin depolymerization with an NaOH loading rate of 2 wt% of the whole slurry [2]. For the current state-of-the-art scenario, we calculated that 26.7% of lignin is converted into aromatics, including *p*-coumaric acid, ferulic acid, and vanillic acid, based on the lignin solubilization rate [17] reported in a prior study and lignin depolymerization data from previous works [2,42]. The depolymerized slurry is then directed to the indigoidine bioconversion unit.

In the bioconversion reactor, *Pseudomonas putida* metabolizes lignin monomers to produce a blue dye (indigoidine) inside the microbial cell. A separate aerobic bioconversion reactor is used for this process similar to isoprenol (Fig. 1). Theoretically, approximately 99 g of indigoidine can be produced from 100 g of lignin monomers [41]. This process

requires a substantial amount of nitrogen when compared to isoprenol production in *E. coli*, which is supplied in the form of ammonium sulfate. After bioconversion, the solid and liquid fractions of the slurry are separated by vacuum filtration. The filtrate is routed to the wastewater treatment unit, while the remaining solid fraction is sent to the cell lysis unit.

In the cell lysis process, tetrahydrofuran (THF) is added as it helps break down the cell mass and it is easier to recover due to its low boiling point of 66 °C [6]. After cell lysis, the cell mass is separated using another vacuum filtration and sent to the onsite energy generation unit. During this filtration, additional THF is used to wash the cell mass instead of water, minimizing the loss of indigoidine with the solid microbial cake. The washed materials are then mixed with the filtrate. The indigoidine-solvent mixture is sent to a distillation unit to recover THF, followed by a successive evaporator to remove water and residual solvent impurities. The waste materials are delivered to the wastewater treatment unit, while the purified indigoidine is stored onsite.

The wastewater treatment, onsite energy generation, and utility stages are developed based on methods and assumptions documented in prior studies [4]. A combination of anaerobic and subsequent aerobic wastewater treatments used in this study recovers clean process water, which is then utilized in the upstream processes, including biomass deconstruction and bioconversion. The solid waste is sent to the landfill for disposal, with a disposal cost of $42.13 per metric ton assigned in the process model [2].

Additionally, the anaerobic treatment of wastewater generates biogas primarily from unutilized sugars. The biogas, along with the remaining solid fraction of biomass and makeup natural gas, is burned in a boiler to generate process steam. Any process steam produced in excess of the biorefinery's demand is sent to the turbo-generator to produce electricity. The solid waste, such as ash, produced in the boiler is handled similarly to the solid waste from the wastewater treatment stage.

Finally, the utility section provides the necessary cooling water, chilled water, and process water to the entire plant. This stage includes a groundwater pumping system, cooling water tower, and chilled water system. Assumptions for these units are consistent with those from previous studies [2,4].

Table 1 summarizes the major data inputs for ensiled biomass sorghum conversion to isoprenol, DMCO, and indigoidine. In addition to these single-point values, the ranges, standard deviations, and probability distributions used to model key input parameters are provided in Supporting Information (Table S1). These ranges were used for sensitivity and uncertainty analyses to better reflect industrial-scale variability.

Table 1
Major data inputs for ensiled biomass sorghum conversion to isoprenol, DMCO, and indigoidine.

Parameters	Units	State-of-the-art scenario[φ]	Optimal future case	Parameters	Units	State-of-the-art scenario[φ]	Optimal future case
Biomass feedstock supply				**Isoprenol bioconversion in *E. coli***			
Biorefinery size[α]	bdt/day			Bioconversion time [19]	h	63.0	36.0
Feedstock cost [16]	$/bdt	101.8	89.5	Glucose-to-isoprenol [19]	wt%	14.0	30.3
CO_{2e} emissions [16]	$kgCO_{2e}$/bdt	130.2	112.6	Xylose-to-isoprenol[θ]	wt%	12.6	27.2
Soil organic carbon sequestration [43]	$kgCO_{2e}$/bdt	−46.0	−80.0	**Indigoidine bioconversion in *P. putida***			
Moisture [16]	%	60.0	60.0	Bioconversion time [23,41]	h	144.0	48.0
Biomass composition [44]				Glucose-to-indigoidine [41]	wt%	33.0	63.24
Cellulose	wt%	30.0	35.0	Xylose-to-indigoidine [45]	wt%	32.0	66.96
Hemicellulose	wt%	15.0	18.0	Lignin-to-indigoidine [23]	wt%	73.91	88.99
Lignin	wt%	20.0	15.0	**Isoprenol upgrading to DMCO** [22,40]			
Lactic acid	wt%	4.8	8.0	Isoprenol-to-isoprene	%	95.0	98.0
Acetic acid	wt%	2.7	3.0	Isoprene dimerization (DMCOD)	%	90.0	98.0
Biomass deconstruction [44]				Isoprene recovery	%	98.0	99.0
Solid loading rate	wt%	30.0	30.0	DMCOD to DMCO isolated yield	wt%	97.0	98.0
Ionic liquid (IL) loading	wt%	5.0	2.5	Hydrogen mixing rate	mg/g-oil	2.94	2.94
IL cost	$/kg	2.0	0.5	Hydrogenation catalyst loading	wt%	0.75	0.75
Lignin to soluble lignin	%	36.5	16.0	**Recovery and separation**			
Enzyme loading rate	mg/g-glucan	10.0	7.0	Product recovery[γ]	%	95.0	98.0
Cellulose to glucose	%	91.5	98.0	IL-recovery[γ]	%	97.0	99.0
Xylan to xylose	%	71.6	95.0	Tetrahydrofuran loading rate[ϕ]	%	50.0	40.0
Hydrolysis time	h	48.0	36.0	Tetrahydrofuran loss[γ]	%	2.0	1.0
Lignin depolymerization				Tetrahydrofuran cost [46]	$/kg	3.3	2.0
NaOH loading rate [2]	%	2.0	2.0	Organic acid recovery[γ]	%	95.0	98.0
Lignin to lignin monomers[β]	%	26.7	55.0	**Equivalent product credits**			
[φ]State-of-the-art scenario considers demonstrated yield of simple sugars and lignin monomers as well as their conversion rates demonstrated at the bench-scale.				Gasoline price [47]	$/L	0.59	0.59
[α]Assumed for analysis in this study similar to economies of scale as determined in prior studies [4].				Jet fuel price [48]	$/L	0.60	0.60
[θ]The isoprenol yield from xylose is assumed to be 90% of the yield reported for glucose.				Synthetic Indigo price[*] [49–51]	$/kg	5.74	5.74

[β] Monomer yield is calculated based on the mass balance data reported in a prior modeling study [2], a range of experimental monomer yields summarized in a previous review [42], and similar work [52] conducted by JBEI researchers on ionic liquid-pretreated biomass. We considered the conversion of soluble lignin after ionic liquid pretreatment (32% of the initial lignin [17]) of 53% and a range of 8–20% conversion of the remaining lignin to monomers [2,42], yielding an average of 26.7% conversion of the initial lignin to monomers.

[γ] Assumed for analysis in this study similar to the product recovery assumed in prior studies [2,4,6].

[ϕ] Assumed for this analysis based on loading rates reported for similar solvents [6].

[*] The price of natural (plant-based) indigo averages $228/kg, ranging from $15 to $1058/kg [49,50].

2.2. Modeling an optimal future case

Compared to the state-of-the-art design discussed in the previous section, we also developed a scenario that pushes each performance metric to its practical limit. This optimal future case scenario provides insight into the lowest achievable cost. This scenario considers a large-scale biorefinery of 3000 bdt/day, along with near-theoretical limits of sugar yield and sugar and lignin conversion rates (Table 1 **and Supplemental Table S1**). While increasing the size of the biorefinery provides the advantage of economies of scale, feedstock supply costs and associated lifecycle CO_2 emissions follow a reverse economy of scale. The lower costs and lifecycle CO_2 emissions from biomass sorghum production and the supply chain in the future case, relative to the state-of-the-art scenario, are due to higher biomass yields (28 bdt/ha) [30], sustainable farming practices with lower nutrient application, and best management practices to reduce truck waiting and handling times [16]. The detailed inputs are documented in our prior work [16].

This optimal future case should be interpreted as an aspirational upper-bound scenario representing best-case process performance and system efficiency, rather than a near-term industrial outcome. It is used to explore theoretical limits and identify key performance drivers under highly optimistic but transparent assumptions.

Our model captures the impacts of variations in biorefinery size and other capital and operating parameters with high fidelity while computing the material and energy balances, as well as capital and operating cost estimations. This allows the use of the same baseline process model with different sets of parameters.

2.3. Determination of minimum selling price and net profit

After performing material and energy balance analyses, capital and operating costs were determined. We adjusted the cost of each process equipment gathered from previous studies based on the new size and scaling exponent. Each equipment cost was further adjusted to 2020 (analysis year) USD using the plant cost index, after which the capital cost was determined. The cost factors used to determine the total capital cost were consistent with prior studies. The annual operating cost includes biomass feedstock cost, costs of process chemicals, waste disposal cost, utility cost, and other fixed operating costs (labor, maintenance, property taxes, and insurance).

The minimum selling price of each product (i.e., isoprenol, DMCO, and indigoidine) was determined using discounted cash flow rate of return (DCFROR) analysis and compared with petroleum-based equivalents. For each product, the total revenue generated from the remaining products and/or coproducts—sold at the current market prices (Table 1)—was assigned as credit. We considered an internal rate of return (IRR) after taxes of 10%, a biorefinery lifetime of 30 years, operating hours of 7920 h (330 days/year and 24 h/day), and an income tax rate of 21% [2,53]. Other economic evaluation parameters used for the DCFROR analysis are consistent with previous techno-economic studies [4].

In addition, policy incentives in this analysis are applied at the product level rather than being explicitly tied to specific feedstocks or regions, in order to maintain general applicability of the framework. We include scenarios in which jet fuels receive a 50% higher subsidy relative to non-jet fuels, consistent with the original design of the Inflation Reduction Act (IRA) 45Z clean fuel tax credit [54], and reflective of additional policy support mechanisms specific to renewable jet fuels (e.g., Carbon Offsetting and Reduction Scheme for International Aviation (CORSIA) [55]). While it is beyond the scope of this study to replicate the full complexity of methodologies used to determine exact incentive values, we apply a simplified range of incentive levels (e.g., on the order of $3/gal for isoprenol and DMCO, with an additional 50% premium for DMCO) that reasonably approximates real-world policy signals. Variations in product prices and the extent to which indigoidine displaces synthetic indigo dye are also evaluated to capture uncertainty. Region-specific incentives (e.g., for lignin valorization) are not explicitly modeled and may influence applicability depending on local policy contexts.

We define the annual net profit as the difference between total revenue and the sum of all expenses and income tax. Total revenue is determined by selling all products and coproducts—including isoprenol, DMCO, indigoidine, organic acids, and onsite electricity (beyond the facility's own use)—at their market prices (Table 1 **and Supplementary Table S1**). The total annual cost is the sum of the annuitized capital cost and annual operating costs. Income tax is determined by calculating taxable income and applying an income tax rate of 21% [2]. Taxable income is calculated as the difference between gross revenue and the sum of production costs, loan interest, depreciation, and prior year losses. The annual net profit is then divided by the annual bone-dry metric tons of biomass utilized at the biorefinery to determine the annual net profit per metric ton of biomass feedstock.

2.4. Lifecycle CO_2-equivalent emissions

Material and energy inputs from the feedstock supply model and biorefinery process model in SuperPro Designer were used to evaluate lifecycle CO_2 emissions footprint. Lifecycle CO_2 impact vectors for these materials and energies were obtained from published LCA databases [56,57]. The LCA model calculates the total carbon footprint by considering the input-output matrix for all relevant inputs and their associated lifecycle CO_2 impact vectors.

For the multiproduct biorefinery considered in this study, coproduct handling for carbon footprint evaluation is complex, as the conventional system expansion method can lead to ambiguous results, such as large negative carbon footprints. Therefore, two approaches were used to calculate the carbon footprint.

The first approach, the system displacement method, determines coproduct credits by displacing equivalent petroleum-based products. Carbon credits for onsite electricity are calculated by displacing grid electricity (U.S. electricity mix), while credits for organic acids, indigoidine, isoprenol, and DMCO are determined by displacing petroleum-based counterparts (except lactic acid). Lactic acid from biomass ensiling replaces corn stover-derived lactic acid, as it is primarily produced through microbial fermentation. While mass, energy, and economic allocations are potential options for allocating the carbon footprint among products and coproducts, this study excludes them due to the diversity of product uses, values, and market demands.

The second approach evaluates the total lifecycle CO_2 emissions reduction relative to petroleum. It calculates the lifecycle CO_2 emissions of the entire biorefinery without allocating emissions to specific products, then compares these emissions to those of a petroleum refinery producing equivalent products and coproducts. This approach is considered more accurate in reflecting the overall lifecycle CO_2 emissions reduction from producing bioproducts compared to petroleum-based products.

2.5. Uncertainty analysis

We evaluated uncertainties in the selling prices and carbon footprints of isoprenol, DMCO, and indigoidine by fitting probability distributions to all input parameters (**Supplementary Table S1**). The selection of probability distributions was based on the nature of the inputs and data availability, as documented in our recent study [53].

3. Results and discussion

3.1. Affordable biofuels and biochemicals at various product ratios

Fig. 2 shows the minimum selling prices at different product ratios, determined through rigorous material and energy balance analyses, accounting for their impacts on capital and operating costs. The results

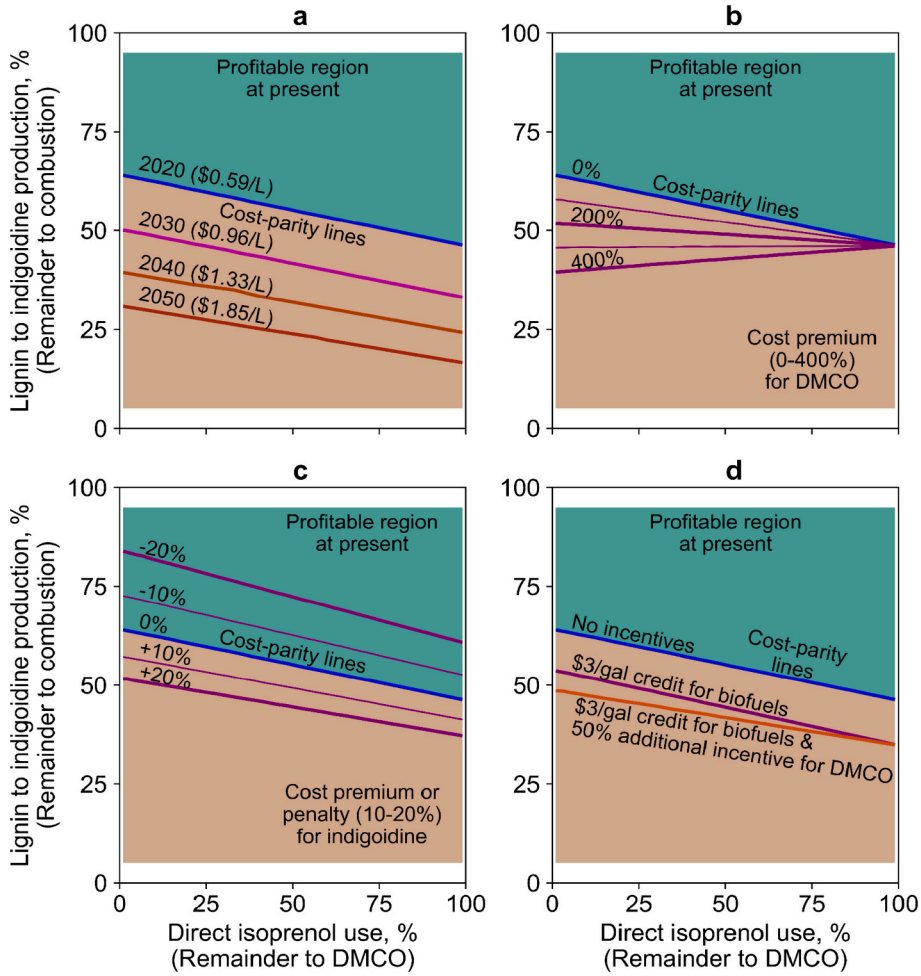


Fig. 2. Cost parity at the current state-of-the-art with various isoprenol and lignin allocations. **(a)** Cost parity with average market prices of gasoline ($0.59/L) [47], jet fuel ($0.60/L) [48], and synthetic indigo dye ($5.74/kg), as well as the projected selling prices of them. The projected gasoline and jet fuel prices in the years 2030, 2040, and 2050 are sourced from the Annual Energy Outlook 2023 [58], while the future price of indigoidine is estimated based on a 2% inflation rate. **(b)** Cost parity with a cost premium of 0–400% for 1,4-dimethylcyclooctane (DMCO). This premium is used solely to determine the threshold at which increased DMCO production becomes economically favorable relative to isoprenol. **(c)** Cost parity with a cost premium and penalty of 0–20% for indigoidine, used to assess the sensitivity of results to fluctuations in indigoidine price. **(d)** Cost-parity with incentive for both isoprenol and DMCO of $3/gal and additional 50% incentive for DMCO due to a high energy-density (9.2% higher than Jet-A). All costs, including the projected selling prices of gasoline, jet fuel, and synthetic indigo dye, are expressed in 2020$.

reveal a wide range of possibilities for achieving price parity for isoprenol, DMCO, and indigoidine with their petroleum counterparts, even at the currently demonstrated yields in bench-scale experiments, provided the yields remain unchanged at the commercial scale. Maximizing direct isoprenol use requires diverting at least 46.8% of lignin to indigoidine production to reach price parity with 2020 market prices (Fig. 2a and b). This threshold decreases with higher petroleum fuel prices, synthetic indigoidine prices, or policy incentives. For example, aligning with 2050 petroleum prices reduces lignin diversion to 17.2% (Fig. 2a), while a 20% increase in synthetic indigoidine prices lowers the threshold to 37.6% (Fig. 2c). A policy incentive of $3/gal reduces the lignin threshold to 35.2% (Fig. 2d). Conversely, maximizing DMCO production requires at least 1.4 times more lignin to be converted to indigoidine (Fig. 2a and b) than in the direct isoprenol use scenario to achieve price parity with petroleum.

Current market dynamics favor the direct use of isoprenol, as increasing DMCO production requires a higher lignin conversion to indigoidine. However, if the price premium for DMCO is increased to three times the current market price of petroleum jet fuel of $0.6/L [48], the biorefinery can produce more DMCO than isoprenol (Fig. 2b). This also holds true when no incentives are provided for isoprenol and a $4.5/gal incentive is given only for DMCO. A higher premium for DMCO is possible because it has a 9.2% higher energy density than Jet-A [22], which either reduces fuel costs for passenger or freight transport or increases flight range, providing substantial benefits to the end users. For instance, replacing conventional Jet-A entirely with DMCO allows an airline to save 46.5 L of fuel per passenger (a 10.3% reduction compared to Jet-A) on a typical international flight from San Francisco (SFO), United States, to London (LHR), United Kingdom [40].

3.2. *Lifecycle CO_2 emissions implications at various product ratios*

Fig. 3 presents the overall CO_2 emissions reduction from a multi-product biorefinery by comparing its total emissions to those of an equivalent petroleum refinery producing the same products. This method does not allocate emissions to specific products but instead calculates total lifecycle CO_2 emissions for producing a set of products. Overall, the modeled biorefinery achieves an average lifecycle CO_2 emissions reduction of 30% at the current state of technology, with greater reductions achieved by increasing direct isoprenol use and reducing lignin diversion to indigoidine (Fig. 3). This is primarily because diverting isoprenol to DMCO production requires additional

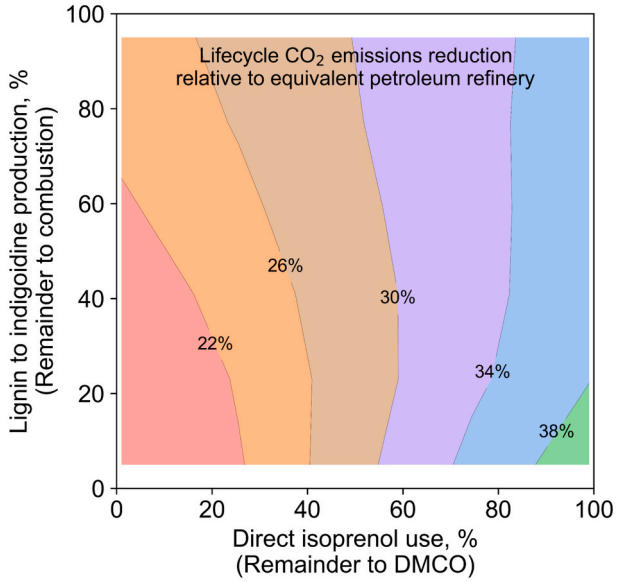


Fig. 3. Lifecycle CO_2 emissions reduction from a biorefinery producing multiple products, including isoprenol, DMCO, indigoidine, organic acids, and electricity, relative to a petroleum refinery producing an equivalent amount of those products.

material and energy inputs while simultaneously reducing the final product yield. In addition, increasing lignin diversion to indigoidine production raises the makeup natural gas to meet the facility's heat and electricity demands, thereby increasing associated emissions.

System expansion is a widely applied method for determining lifecycle CO_2 emissions, endorsed by the Intergovernmental Panel on Climate Change (IPCC) [59,60] and incorporated into biofuel policies around the world [60,61]. Under this framework, we observe highly favorable lifecycle CO_2e reductions that vary according to which product is treated as the primary output (**Supplemental Fig. S1**), highlighting the challenges of applying system expansion to complex multiproduct biorefineries. Supplemental **Fig. S1** demonstrates that adjusting product ratios can create substantial opportunities to achieve carbon-neutral biofuels. Although high coproduct output can support carbon-neutral or even carbon-negative performance, biorefineries must balance cost and emissions, as allocating more carbon to the primary product generally reduces production costs. Thus, strategic adjustment of product ratios provides a flexible means to optimize both economic performance and lifecycle CO_2 emissions.

3.3. Comparing uncertainty in minimum selling price across multiproduct and standalone biorefineries

The increased number of input variables in the modeled multiproduct biorefinery results in greater uncertainty in the selling prices of isoprenol, DMCO, and indigoidine compared to when they are produced in standalone biorefineries (Fig. 4). This highlights the challenges of managing a multiproduct biorefinery, especially when uncertainty exists in raw material use, energy consumption, product yield, and market conditions. However, while the technical complexity of multiproduct biorefineries increases risk, the increased number of products also enables risk reduction through diversification, provided the prices of all products are not strongly correlated.

The results show a 20–30% likelihood of isoprenol, DMCO, and indigoidine selling prices reaching cost parity with their petroleum counterparts when produced together. Achieving price parity when each of the fuel molecules is produced individually remains highly challenging; although the lower bound of the isoprenol minimum selling price approaches gasoline parity under optimistic assumptions, sustained cost competitiveness is unlikely without substantial process intensification beyond conventional optimization. We observed greater uncertainty when allocating more isoprenol to DMCO. This was mainly due to uncertainty in the isoprenol-to-DMCO conversion rate as the

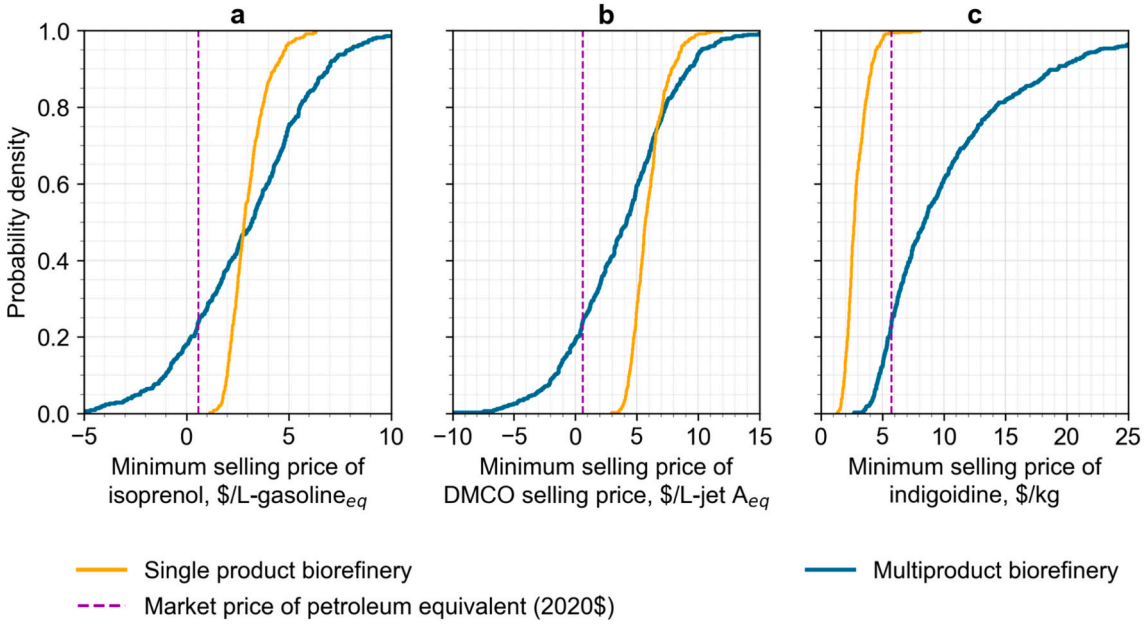


Fig. 4. Uncertainties in the minimum selling price of isoprenol, DMCO, and indigoidine at the current state of technology, produced in multiproduct and standalone biorefineries.

(a) Uncertainties in the minimum selling price of isoprenol. (**b**) Uncertainties in the minimum selling price of DMCO. (**c**) Uncertainties in the minimum selling price of indigoidine. In a single-product biorefinery, isoprenol production is solely from sugars (mainly glucose and xylose), while indigoidine production comes from both sugars and lignin-derived intermediates, as *P. putida* can catabolize both sugars and aromatics. For a multiproduct biorefinery, a typical cost-parity point is considered where 50% of isoprenol is retained for direct use as a gasoline blendstock, and the other 50% is diverted to DMCO production as well as 55.2% of lignin is diverted to indigoidine production (Fig. 2-a), with the remainder used for combustion.

technology transitions from the current state of technology to when it is fully optimized. In contrast, indigoidine production showed lower uncertainty. These results highlight that a product with a higher conversion yield results in minimal impact, as the effect per unit of product is small. More importantly, the likelihood of cost parity for indigoidine decreases substantially, from nearly 100% when produced alone to 25% in a multiproduct biorefinery, as sugars are diverted to lower-value products like isoprenol and DMCO. Diverting all biomass carbon sources to large-scale indigoidine production could oversaturate the market unless new applications are explored. Currently, based on the use of petroleum-derived indigo, the primary application of indigoidine appears to be in textile dyeing. However, indigoidine distinguishes itself in this use case through its environmental profile: it mitigates the generation of toxic waste [51] and high chemical demand of synthetic indigo production while avoiding the land-use intensity and yield limitations of natural plant-based indigo cultivation [50].

For both single-product and multiproduct biorefineries, several input parameters substantially contribute to the uncertainty in selling price, particularly those affecting material and energy requirements, product yield, or both. Key contributors from biomass production and supply include biomass yield, supply radius, organic acid generation during ensiling, and biomass quality at the pretreatment reactor throat, primarily determined by carbohydrate and lignin content. In the biomass pretreatment, hydrolysis, and lignin depolymerization stages, uncertainty in model predictions arises primarily from variability in process parameters, including ionic liquid loading and recovery rates, enzyme loading rate, and glucose, xylose, and lignin-derived bio-intermediates yields.

Variability in parameters associated with bioconversion—including sugar-to-isoprenol and lignin intermediate-to-indigoidine conversion

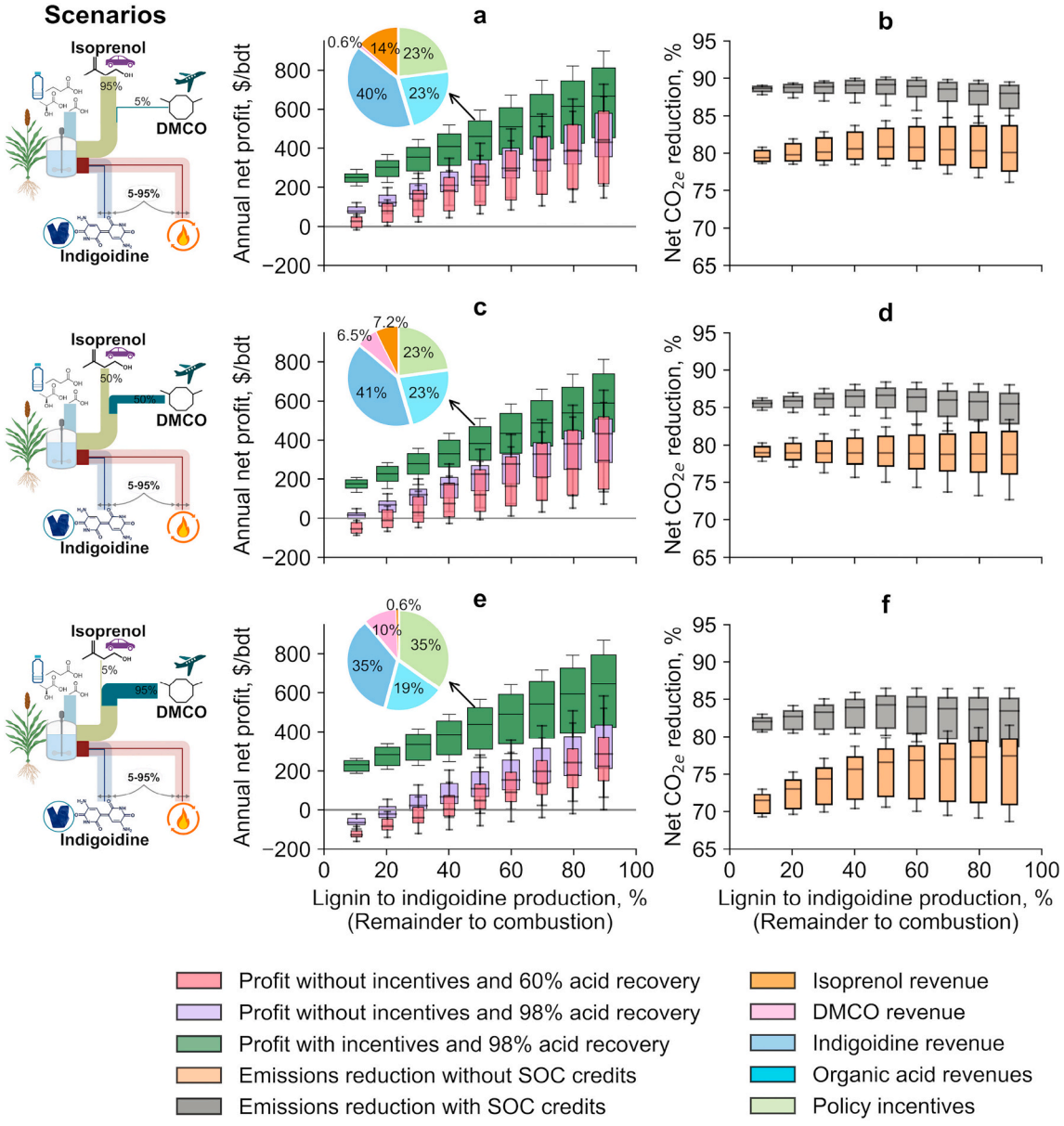


Fig. 5. Uncertainties in annual net profit per bone-dry metric ton of biomass and lifecycle CO_2 emissions reduction under the optimal future case scenario. **Figures (a), (c), and (e)** illustrate the annual net profit per bone-dry metric ton (bdt) of biomass feedstock with or without policy incentives, at isoprenol retention rates of 95%, 50%, and 5%, respectively, as well as their corresponding overall carbon footprint reductions from the biorefinery relative to a petroleum refinery producing equivalent products are shown in Figures **(b), (d), and (f)**, respectively. The box plot illustrates uncertainties arising from the uncertainty in the selling price ($3–10/kg) and carbon footprint (4–13.8 $kgCO_{2e}$/kg) of synthetic indigo dye. This study includes incentive for both isoprenol and DMCO of $3/gal and additional 50% incentive for DMCO due to a high energy-density biofuel (9.2% higher than Jet-A). CO_{2e} represents lifecycle CO_2 equivalent emissions.

yields, bioconversion time, and bioreactor energy consumption (e.g., agitation)—substantially affects the minimum selling price of the product. Implementing advanced bioreactor designs, such as bubble column reactors with optimized oxygen supply and mixing, can help mitigate these effects. Similarly, conversion yields at each stage of isoprenol-to-DMCO upgrading—a three-stage process—are critical factors influencing the minimum selling price. Addressing these sources of variability through process optimization and technological improvements is essential to enhance economic viability.

3.4. Lignin utilization thresholds for profit and carbon reduction

Lignin conversion to value-added biochemicals or biomaterials is a major topic of interest in current research. Here, we first demonstrate how lignin conversion to indigoidine impacts biorefinery process economics and lifecycle CO_2 emissions, using a multiproduct biorefinery as a representative example (Fig. 5). We created three different biorefinery configurations by adjusting the ratios of two major biofuels, isoprenol and DMCO, and considered process parameters optimized to reach 90% of the theoretical biomass-to-product yield. Results show that the impact of lignin-derived products is highly specific to biorefinery configurations (See Fig. 5).

For the isoprenol-rich biorefinery configuration, only 5% of lignin allocation to indigoidine production is sufficient to generate net profit without any policy incentives. Key parameters impacting this threshold include variabilities in indigoidine price, the amount of indigoidine required for functional displacement, and the purity or recovery of industrial-grade organic acids. For instance, at a low indigoidine selling price of $3/kg and a 60% recovery rate of high-purity organic acids, 20% of lignin must be allocated to indigoidine production. Policy incentives for both isoprenol and DMCO can offset revenue losses. In fact, even without indigoidine production, the biorefinery can generate a net profit if industrial-grade organic acids are recovered.

The value and purity of organic acids and indigoidine consistently impact the net profit of other biorefinery configurations. Biorefinery configurations with 50% and 5% of isoprenol allocated for direct use require at least 9.5% and 26.6% of lignin allocation to indigoidine production, respectively, to generate a net profit without policy incentives. In a conservative scenario with a low indigoidine selling price of $3/kg and a 60% industrial-grade organic acid recovery rate, these configurations require at least 50% and 90% lignin allocation to indigoidine, respectively. This highlights the importance of lignin valorization for biofuels requiring intensive conversion steps. In such cases, producing high-energy-density products like DMCO adds value to the biorefinery by either providing performance advantages or generating incentives.

With policy incentives of $0.8/L ($3/gal) for isoprenol and $1.2/L ($4.5/gal) for DMCO, a multiproduct biorefinery with selected product ratios can generate an average net profit of $382–$467/bdt ($111–$252/bdt without policy incentives), with 50% lignin allocation to indigoidine (Fig. 5). This net profit increases with higher lignin utilization. A 50% lignin utilization is highly feasible, as the biorefinery can generate net profit across a wide range of isoprenol and DMCO ratios. Even in a conservative scenario with a low indigoidine selling price of $3/kg and a 60% industrial-grade organic acid recovery rate, the average net profit ranges from $55–$236/bdt with 50% lignin allocation to indigoidine.

Results show that lignin allocation to indigoidine up to 50% is generally beneficial for lifecycle CO_2 emissions reduction. However, further diverting lignin to indigoidine leads to increased lifecycle CO_{2e} emissions in the biorefinery due to higher use of supplemental natural gas for heat and power. Unlike the minimum selling price, the multiproduct biorefinery consistently achieves an overall lifecycle CO_2 emissions reduction of 70–80% without SOC benefits and 80–88% with SOC benefits, with a higher reduction observed when the biorefinery produces a larger fraction of isoprenol.

4. Conclusions

Converting a single biomass stream into bio-based gasoline, jet fuel, and platform chemicals presents substantial opportunities for flexible product allocation, enabling economically viable and low-carbon outcomes. In this study, we evaluated conditions under which biorefineries can achieve price parity with commercial alternatives at currently demonstrated yields, provided high recovery of organic acids is maintained and biomass-to-product conversion approaches theoretical maxima. Our analysis shows that for a typical allocation of 50% isoprenol and 50% lignin by mass, the modeled biorefinery can achieve a net annual profit exceeding $123 per bone-dry ton of biomass, alongside a greenhouse gas emissions reduction of over 75%, increasing to more than 84% when soil organic carbon sequestration is included. Organic acids generated during biomass ensiling, including acetic acid, lactic acid, and butyric acid, contribute significantly to both economic performance and life cycle emissions benefits, although challenges remain in recovering industrial-grade acids due to their similar boiling points. High-value co-products such as pigments (e.g., indigoidine) provide additional revenue streams compared to low-value fuel blendstocks (isoprenol and DMCO), with potential applications in textile dyeing, food coloring, and bioelectronics, emphasizing the importance of diversified markets. Efficient microbial conversion of real biomass-derived intermediates, including sugars and lignin-derived compounds, remains a key bottleneck for scale-up, as laboratory demonstrations rely on specialty pure chemicals. Catalytic upgrading of isoprenol to DMCO, while validated at small scale, also requires commercial demonstration. Nevertheless, the analysis indicates that multiproduct biorefineries can generate strong profitability across a range of product ratios and market scenarios, leveraging lignin and carbohydrate streams to optimize both economic and environmental performance. Overall, the results highlight the feasibility of a scalable, adaptive biomanufacturing framework in which versatile platform chemicals and co-products derived from a single biomass feedstock enable substantial lifecycle CO_{2e} reductions, economic resilience, and enhanced sustainability of biofuel and biochemical production.

CRediT authorship contribution statement

Nawa Raj Baral: Writing – original draft, Validation, Methodology, Formal analysis, Conceptualization. **Thomas Eng:** Writing – review & editing, Methodology, Data curation. **Deepanwita Banerjee:** Writing – review & editing, Methodology, Data curation. **Blake A. Simmons:** Writing – review & editing. **Aindrila Mukhopadhyay:** Writing – review & editing. **Corinne D. Scown:** Writing – review & editing, Validation, Conceptualization.

Declaration of competing interest

N.R.B and B.A.S. have a financial interest in Erg Bio. B.A.S. also has a financial interest in Caribou Biofuels and Illium Technologies. C.D.S. has a financial interest in Cyklos Materials.

Acknowledgments

This material is based upon work at the Joint BioEnergy Institute supported by the U.S. Department of Energy, Office of Science, Biological and Environmental Research Program under Contract Number DE-AC02-05CH11231 between Lawrence Berkeley National Laboratory and the U.S. Department of Energy. This material is also based upon work supported by the Defense Advanced Research Projects Agency (DARPA). Additionally, this study was supported by the U.S. Department of Energy, Critical Minerals and Energy Innovation, Bioenergy Technologies Office. The United States Government retains and the publisher, by accepting the article for publication, acknowledges that the United States Government retains a nonexclusive, paid-up,

irrevocable, worldwide license to publish or reproduce the published form of this manuscript, or allow others to do so, for United States Government purposes. The views, opinions and/or findings expressed are those of the author and should not be interpreted as representing the official views or policies of the U.S. Department of Energy, the U.S. Department of Defense or the U.S. Government. The graphical abstract and Figure 1 were generated with Biorender (https://BioRender.com).

Appendix A. Supplementary data

Detailed operating data inputs for the current state of technology and optimal future case scenarios—including their minimum and maximum values and the probability distributions used in this study—are provided in the supplementary information. Additionally, the supplementary information includes lifecycle CO_2 emissions associated with process chemicals, energy sources, and coproducts. Supplementary information related to this article can be found online at https://doi.org/10.1016/j.cej.2026.177641.

Data availability

Process flowsheet, equipment sizing, equipment costing, and the standard JSON file of modeling data are available at https://projectpisces.org/flowsheets/297. Any other specific process modeling inputs and metabolic modeling data are available from the lead contact upon request.

References

[1] National Security Commission on Emerging Biotechnology Urges Swift Action to Protect U.S. National Security - Biotech, (2025). https://www.biotech.senate.gov/press-releases/nsceb-publishes-final-report/ (accessed January 6, 2026).

[2] R.E. Davis, N.J. Grundl, L. Tao, M.J. Biddy, E.C. Tan, G.T. Beckham, D. Humbird, D.N. Thompson, M.S. Roni, Process design and economics for the conversion of lignocellulosic biomass to hydrocarbon fuels and coproducts: 2018 biochemical design case update; biochemical deconstruction and conversion of biomass to fuels and products via integrated biorefinery pathways, National Laboratory of the Rockies (NLR), Golden, CO (United States), 2018. https://doi.org/https://doi.org/10.2172/1483234.

[3] D.M. Alonso, S.H. Hakim, S. Zhou, W. Won, O. Hosseinaei, J. Tao, V. Garcia-Negron, A.H. Motagamwala, M.A. Mellmer, K. Huang, C.J. Houtman, N. Labbé, D. P. Harper, C. Maravelias, T. Runge, J.A. Dumesic, Increasing the revenue from lignocellulosic biomass: Maximizing feedstock utilization, Sci. Adv. 3 (2017) e1603301, https://doi.org/10.1126/sciadv.1603301.

[4] D. Humbird, R. Davis, L. Tao, C. Kinchin, D. Hsu, A. Aden, P. Schoen, J. Lukas, B. Olthof, M. Worley, D. Sexton, D. Dudgeon, Process Design and Economics for Biochemical Conversion of Lignocellulosic Biomass to Ethanol: Dilute-Acid Pretreatment and Enzymatic Hydrolysis of Corn Stover, National Laboratory of the Rockies (NLR), Golden, CO (United States) (2011), https://doi.org/10.2172/1013269.

[5] A.O. Ojo, O. de Smidt, Lactic acid: A comprehensive review of production to purification, Processes 11 (2023) 688, https://doi.org/10.3390/pr11030688.

[6] N.R. Baral, D. Banerjee, T. Eng, B.A. Simmons, A. Mukhopadhyay, C.D. Scown, Microbial Pathways for Cost-Effective Low-Carbon Renewable Indigoidine, ACS Sustain. Chem. Eng. (2025), https://doi.org/10.1021/acssuschemeng.4c09962.

[7] A.W. Bartling, M.L. Stone, R.J. Hanes, A. Bhatt, Y. Zhang, M.J. Biddy, R. Davis, J. S. Kruger, N.E. Thornburg, J.S. Luterbacher, R. Rinaldi, J.S.M. Samec, B.F. Sels, Y. Román-Leshkov, G.T. Beckham, Techno-economic analysis and life cycle assessment of a biorefinery utilizing reductive catalytic fractionation, Energy Environ. Sci. 14 (2021) 4147–4168, https://doi.org/10.1039/D1EE01642C.

[8] M. Jahangeer, M.U. Rehman, R. Nelofer, M. Nadeem, B. Munir, W. Smułek, T. Jesionowski, S.A. Qamar, Biotransformation of Lignocellulosic Biomass to Value-Added Bioproducts: Insights into Bio-Saccharification Strategies and Potential Concerns, Top. Catal. (2024), https://doi.org/10.1007/s11244-024-01941-9.

[9] B. Long, F. Zhang, S.Y. Dai, M. Foston, Y.J. Tang, J.S. Yuan, Engineering strategies to optimize lignocellulosic biorefineries, Nat. Rev. Bioeng. (2024), https://doi.org/10.1038/s44222-024-00247-5.

[10] S. Farzad, M.A. Mandegari, M. Guo, K.F. Haigh, N. Shah, J.F. Görgens, Multi-product biorefineries from lignocelluloses: a pathway to revitalisation of the sugar industry? Biotechnol. Biofuels 10 (2017) 87, https://doi.org/10.1186/s13068-017-0761-9.

[11] S. Liu, D. Wu, D. Sun, Y. Zhang, H. Zhang, T. Ma, S. Wang, Electricity-driven CO2 and biomass conversion toward formic acid/formate: microenvironment regulation, hydrogen storage potential, and sustainability assessment, Energy Environ. Sci. 19 (2026) 1837–1898, https://doi.org/10.1039/D5EE07819A.

[12] S. Nitopi, E. Bertheussen, S.B. Scott, X. Liu, A.K. Engstfeld, S. Horch, B. Seger, I.E. L. Stephens, K. Chan, C. Hahn, J.K. Nørskov, T.F. Jaramillo, I. Chorkendorff, Progress and perspectives of electrochemical CO2 reduction on copper in aqueous electrolyte, Chem. Rev. 119 (2019) 7610–7672, https://doi.org/10.1021/acs.chemrev.8b00705.

[13] L. He, L. Zhang, H. Zhou, Y. Nie, H. Wang, B. Tang, H. Li, T. Ma, H. Zhang, Boosting Photocatalytic Upcycling of Liquid Biomass into Biodiesel via Microenvironment Modulation, Adv. Energy Mater. 15 (2025), https://doi.org/10.1002/aenm.202403168.

[14] M. Yang, D. Liu, N.R. Baral, C.-Y. Lin, B.A. Simmons, J.M. Gladden, A. Eudes, C. D. Scown, Comparing in planta accumulation with microbial routes to set targets for a cost-competitive bioeconomy, Proc. Natl Acad. Sci. USA 119 (2022) e2122309119, https://doi.org/10.1073/pnas.2122309119.

[15] M. Yang, N.R. Baral, B.A. Simmons, J.C. Mortimer, P.M. Shih, C.D. Scown, Accumulation of high-value bioproducts in planta can improve the economics of advanced biofuels, Proc. Natl Acad. Sci. USA 117 (2020) 8639–8648, https://doi.org/10.1073/pnas.2000053117.

[16] N.R. Baral, J. Dahlberg, D. Putnam, J.C. Mortimer, C.D. Scown, Supply cost and life-cycle greenhouse gas footprint of dry and ensiled biomass sorghum for biofuel production, ACS Sustain. Chem. Eng. 8 (2020) 15855–15864, https://doi.org/10.1021/acssuschemeng.0c03784.

[17] H.D. Magurudeniya, N.R. Baral, A. Rodriguez, C.D. Scown, J. Dahlberg, D. Putnam, A. George, B.A. Simmons, J.M. Gladden, Use of ensiled biomass sorghum increases ionic liquid pretreatment efficiency and reduces biofuel production cost and carbon footprint, Green Chem. 23 (2021) 3127–3140, https://doi.org/10.1039/D0GC03260C.

[18] D. Essien, T.L. Richard, Ensiled wet storage accelerates pretreatment for bioconversion of corn stover, Front. Bioeng. Biotechnol. 6 (2018) 195, https://doi.org/10.3389/fbioe.2018.00195.

[19] A. Kang, D. Mendez-Perez, E.-B. Goh, E.E.K. Baidoo, V.T. Benites, H.R. Beller, J. D. Keasling, P.D. Adams, A. Mukhopadhyay, T.S. Lee, Optimization of the IPP-bypass mevalonate pathway and fed-batch fermentation for the production of isoprenol in Escherichia coli, Metab. Eng. 56 (2019) 85–96, https://doi.org/10.1016/j.ymben.2019.09.003.

[20] J. Wang, T. Jiang, S. Milligan, J. Zhang, C. Li, Y. Yan, Improving isoprenol production via systematic CRISPRi screening in engineered Escherichia coli, Green Chem. 24 (2022) 6955–6964, https://doi.org/10.1039/D2GC02255A.

[21] J. Menasalvas, S. Kulakowski, Y. Chen, J.W. Gin, E. Akyuz Turumtay, N.R. Baral, M.A. Apolonio, A. Rivier, I.S. Yunus, M.E. Garber, C.D. Scown, P.D. Adams, T. S. Lee, I.K. Blaby, E.E.K. Baidoo, C.J. Petzold, T. Eng, A. Mukhopadhyay, Biosensor-driven strain engineering reveals key cellular processes for maximizing isoprenol production in Pseudomonas putida, Sci. Adv. 11 (2025) eady2677, https://doi.org/10.1126/sciadv.ady2677.

[22] K.E. Rosenkoetter, C.R. Kennedy, P.J. Chirik, B.G. Harvey, [4 + 4]-cycloaddition of isoprene for the production of high-performance bio-based jet fuel, Green Chem. 21 (2019) 5616–5623, https://doi.org/10.1039/C9GC02404B.

[23] T. Eng, D. Banerjee, J. Menasalvas, Y. Chen, J. Gin, H. Choudhary, E. Baidoo, J. H. Chen, A. Ekman, R. Kakumanu, Y.L. Diercks, A. Codik, C. Larabell, J. Gladden, B.A. Simmons, J.D. Keasling, C.J. Petzold, A. Mukhopadhyay, Maximizing microbial bioproduction from sustainable carbon sources using iterative systems engineering, Cell Rep. 42 (2023) 113087, https://doi.org/10.1016/j.celrep.2023.113087.

[24] W.N. Cude, J. Mooney, A.A. Tavanaei, M.K. Hadden, A.M. Frank, C.A. Gulvik, A. L. May, A. Buchan, Production of the antimicrobial secondary metabolite indigoidine contributes to competitive surface colonization by the marine roseobacter Phaeobacter sp. strain Y4I, Appl. Environ. Microbiol. 78 (2012) 4771–4780, https://doi.org/10.1128/AEM.00297-12.

[25] C. Yumusak, A.J. Prochazkova, D.H. Apaydin, H. Seelajaroen, N.S. Sariciftci, M. Weiter, J. Krajcovic, Y. Qin, W. Zhang, J. Zhan, A. Kovalenko, Indigoidine – Biosynthesized organic semiconductor, Dyes Pigments 171 (2019) 107768, https://doi.org/10.1016/j.dyepig.2019.107768.

[26] Z. Qin, X. Wang, S. Gao, D. Li, J. Zhou, Production of natural pigments using microorganisms, J. Agric. Food Chem. 71 (2023) 9243–9254, https://doi.org/10.1021/acs.jafc.3c02222.

[27] M.R. Ghiffary, C.P.S. Prabowo, K. Sharma, Y. Yan, S.Y. Lee, H.U. Kim, High-Level Production of the Natural Blue Pigment Indigoidine from Metabolically Engineered Corynebacterium glutamicum for Sustainable Fabric Dyes, ACS Sustain. Chem. Eng. 9 (2021) 6613–6622, https://doi.org/10.1021/acssuschemeng.0c09341.

[28] Project PISCES - Process Integration & Synthesis using Chemical Engineering Standards. https://projectpisces.org/flowsheets/297, 2026. (Accessed 29 April 2026).

[29] Intelligen, SuperPro Designer, Intelligen. https://www.intelligen.com/products/superpro-overview/, 2020. (Accessed 29 April 2026).

[30] T. Huntington, X. Cui, U. Mishra, C.D. Scown, Machine learning to predict biomass sorghum yields under future climate scenarios, Biofuels, Bioprod. Bioref. 14 (2020) 566–577, https://doi.org/10.1002/bbb.2087.

[31] H. Choudhary, B.A. Simmons, J.M. Gladden, Comparative Study on the Pretreatment of Aspen and Maple With 1-Ethyl-3-methylimidazolium Acetate and Cholinium Lysinate, Front. Energy Res. 10 (2022), https://doi.org/10.3389/fenrg.2022.868181.

[32] A. Yao, H. Choudhary, M. Mohan, A. Rodriguez, H. Magurudeniya, J.G. Pelton, A. George, B.A. Simmons, J.M. Gladden, Can multiple ions in an ionic liquid improve the biomass pretreatment efficacy? ACS Sustain. Chem. Eng. 12 (2021) 4371–4376, https://doi.org/10.1021/acssuschemeng.0c09330.

[33] N. Sun, R. Parthasarathi, A.M. Socha, J. Shi, S. Zhang, V. Stavila, K.L. Sale, B. A. Simmons, S. Singh, Understanding pretreatment efficacy of four cholinium and imidazolium ionic liquids by chemistry and computation, Green Chem. 16 (2014) 2546–2557, https://doi.org/10.1039/C3GC42401D.

[34] B. Neupane, N.V.S.N.M. Konda, S. Singh, B.A. Simmons, C.D. Scown, Life-cycle greenhouse gas and water intensity of cellulosic biofuel production using cholinium lysinate ionic liquid pretreatment, ACS Sustain, Chem. Eng. 5 (2017) 10176–10185, https://doi.org/10.1021/acssuschemeng.7b02116.
[35] Q.-Z. Li, X.-L. Jiang, X.-J. Feng, J.-M. Wang, C. Sun, H.-B. Zhang, M. Xian, H.-Z. Liu, Recovery Processes of Organic Acids from Fermentation Broths in the Biomass-Based Industry, J. Microbiol. Biotechnol. 26 (2016) 1–8, https://doi.org/10.4014/jmb.1505.05049.
[36] C.S. López-Garzón, A.J.J. Straathof, Recovery of carboxylic acids produced by fermentation, Biotechnol. Adv. 32 (2014) 873–904, https://doi.org/10.1016/j.biotechadv.2014.04.002.
[37] E.M. Karp, R.M. Cywar, L.P. Manker, P.O. Saboe, C.T. Nimlos, D. Salvachúa, X. Wang, B.A. Black, M.L. Reed, W.E. Michener, N.A. Rorrer, G.T. Beckham, Post-Fermentation Recovery of Biobased Carboxylic Acids, ACS Sustain. Chem. Eng. 6 (2018) 15273–15283, https://doi.org/10.1021/acssuschemeng.8b03703.
[38] J. Sun, J. Shi, N.V.S.N. Murthy Konda, D. Campos, D. Liu, S. Nemser, J. Shamshina, T. Dutta, P. Berton, G. Gurau, R.D. Rogers, B.A. Simmons, S. Singh, Efficient dehydration and recovery of ionic liquid after lignocellulosic processing using pervaporation, Biotechnol. Biofuels 10 (2017) 154, https://doi.org/10.1186/s13068-017-0842-9.
[39] N.R. Baral, O. Kavvada, D. Mendez-Perez, A. Mukhopadhyay, T.S. Lee, B. A. Simmons, C.D. Scown, Production Cost, Water Use, and Greenhouse Gas Footprint of a Bio-Based Long-Chain Alcohol as a Renewable Transportation Fuel, Environ. Sci, Technol, 2019.
[40] N.R. Baral, M. Yang, B.G. Harvey, B.A. Simmons, A. Mukhopadhyay, T.S. Lee, C. D. Scown, Production cost and carbon footprint of biomass-derived dimethylcyclooctane as a high-performance jet fuel blendstock, ACS Sustain. Chem. Eng. 9 (2021) 11872–11882, https://doi.org/10.1021/acssuschemeng.1c03772.
[41] D. Banerjee, T. Eng, A.K. Lau, Y. Sasaki, B. Wang, Y. Chen, J.-P. Prahl, V.R. Singan, R.A. Herbert, Y. Liu, D. Tanjore, C.J. Petzold, J.D. Keasling, A. Mukhopadhyay, Genome-scale metabolic rewiring improves titers rates and yields of the non-native product indigoidine at scale, Nat. Commun. 11 (2020) 5385, https://doi.org/10.1038/s41467-020-19171-4.
[42] W. Schutyser, T. Renders, S. Van den Bosch, S.F. Koelewijn, G.T. Beckham, B. F. Sels, Chemicals from lignin: an interplay of lignocellulose fractionation, depolymerisation, and upgrading, Chem. Soc. Rev. 47 (2018) 852–908, https://doi.org/10.1039/c7cs00566k.
[43] S. Gautam, U. Mishra, C.D. Scown, Y. Zhang, Sorghum biomass production in the continental United States and its potential impacts on soil organic carbon and nitrous oxide emissions, Glob. Change Biol. Bioenergy. 12 (2020) 878–890, https://doi.org/10.1111/gcbb.12736.
[44] H.D. Magurudeniya, A. Rodriguez, N.R. Baral, C.D. Scown, A. George, B. A. Simmons, J.M. Gladden, Ensiled Biomass Increases Ionic Liquid Pretreatment Efficiency and Reduces Biofuel Production Cost and Carbon Footprint, Green Chem. 23 (8) (2020) 3127–3140.
[45] H.G. Lim, T. Eng, D. Banerjee, G. Alarcon, A.K. Lau, M.-R. Park, B.A. Simmons, B. O. Palsson, S.W. Singer, A. Mukhopadhyay, A.M. Feist, Generation of Pseudomonas putida KT2440 strains with efficient utilization of xylose and galactose via adaptive laboratory evolution, ACS Sustain. Chem. Eng. 9 (2021) 11512–11523, https://doi.org/10.1021/acssuschemeng.1c03765.
[46] Tetrahydrofuran Prices | Historical and Current, (n.d.). https://www.intratec.us/chemical-markets/tetrahydrofuran-price (accessed March 11, 2025).
[47] U.S. Total Gasoline Wholesale/Resale Price by Refiners (Dollars per Gallon). https://www.eia.gov/dnav/pet/hist/LeafHandler.ashx?n=PET&s=EMA_EPM0_PWG_NUS_DPG&f=M, 2020. (Accessed 29 January 2025).
[48] E I A, U.S. Kerosene-Type Jet Fuel Wholesale/Resale Price by Refiners, (2020). https://www.eia.gov/dnav/pet/hist/LeafHandler.ashx?n=PET&s=EMA_EPJK_PWG_NUS_DPG&f=M (accessed February 4, 2020).
[49] N. Wenner, The Production of Indigo Dye from Plants. http://www.fibershed.com/wp-content/uploads/2018/08/production-of-Indigo-dye-aug2018-update.pdf, 2017. (Accessed 30 December 2019).
[50] L. Pattanaik, S.K. Padhi, P. Hariprasad, S.N. Naik, Life cycle cost analysis of natural indigo dye production from Indigofera tinctoria L. plant biomass: a case study of India, Clean Techn, Environ. Policy. 22 (2020) 1639–1654, https://doi.org/10.1007/s10098-020-01914-y.
[51] G.N. Bidart, D. Teze, C.U. Jansen, E. Pasutto, N. Putkaradze, A.-M. Sesay, F. Fredslund, L. Lo Leggio, O. Ögmundarson, S. Sukumara, K. Qvortrup, D. H. Welner, Chemoenzymatic indican for light-driven denim dyeing, Nat. Commun. 15 (2024) 1489, https://doi.org/10.1038/s41467-024-45749-3.
[52] H. Choudhary, L. Das, J.G. Pelton, L. Sheps, B.A. Simmons, J.M. Gladden, S. Singh, Funneled Depolymerization of Ionic Liquid-Based Biorefinery "Heterogeneous" Lignin into Guaiacols over Reusable Palladium Catalyst, Chem. Eur. J. 29 (2023) e202300330, https://doi.org/10.1002/chem.202300330.
[53] N.R. Baral, O. Kavvada, D. Mendez-Perez, A. Mukhopadhyay, T.S. Lee, B. A. Simmons, C.D. Scown, Techno-economic analysis and life-cycle greenhouse gas mitigation cost of five routes to bio-jet fuel blendstocks, Energy Environ. Sci. 12 (2019) 807–824, https://doi.org/10.1039/C8EE03266A.
[54] IRA, The Section 45Z Clean Fuel Production Credit, (2022). https://www.congress.gov/crs_external_products/IF/PDF/IF12502/IF12502.2.pdf (accessed April 23, 2026).
[55] ICAO, CORSIA Sustainability Criteria for CORSIA Eligible Fuels. https://www.icao.int/sites/default/files/environmental-protection/CORSIA/Documents/CORSIA%20Eligible%20Fuels/ICAO-document-05-Sustainability-Criteria-June-2025.pdf, 2025. (Accessed 24 April 2026).
[56] Argonne GREET Model. https://greet.es.anl.gov/, 2019. (Accessed 25 January 2021).
[57] ECOINVENT, Ecoinvent LCI database. https://www.ecoinvent.org/, 2019. (Accessed 22 July 2019).
[58] Annual Energy Outlook 2023, U.S. Energy Information Administration (EIA), (2024). https://www.eia.gov/outlooks/aeo/tables_ref.php (accessed January 29, 2025).
[59] ISO 14044:2006 - Environmental management — Life cycle assessment — Requirements and guidelines, (2006). https://www.iso.org/standard/38498.html (accessed January 28, 2026).
[60] F. Pierobon, I.L. Eastin, I. Ganguly, Life cycle assessment of residual lignocellulosic biomass-based jet fuel with activated carbon and lignosulfonate as co-products, Biotechnol. Biofuels 11 (2018) 139, https://doi.org/10.1186/s13068-018-1141-9.
[61] EPA, Overview of the Renewable Fuel Standard Program. https://www.epa.gov/renewable-fuel-standard/overview-renewable-fuel-standard-program, 2025. (Accessed 28 January 2026).